$^{19}F(^3He,d)^{20}Ne$ Reaction at 20–23 MeV*

A. W. Obst† and K. W. Kemper
Department of Physics, The Florida State University, Tallahassee, Florida 32306

(Received 20 July 1973)

14 deuteron groups populating levels to 10.26 MeV excitation in ^{20}Ne have been measured with the ^{19}F $(^3He,d)^{20}Ne$ reaction. Excitation functions measured at $\theta_{lab}=25$ and 45° from 20.0 to 21.2 MeV reveal little structure, and therefore probably little compound-nuclear contribution to the observed cross sections for the deuteron groups. In particular, the 2^- level at 4.97 MeV excitation, strongly populated at $E_{^3He}=10$ MeV, is weakly populated in the present energy range. The "j-forbidden" 4^+ level at 4.25 MeV excitation, on the other hand, is strongly populated in the present energy range. A collective-model coupled-channel Born-approximation analysis of angular distributions measured at $E_{^3He}=21$ and 23 MeV is better able to explain the data than distorted-wave Born-approximation analysis for the positive-parity states. The negative-parity states are poorly described by both theories.

[NUCLEAR REACTIONS ^{19}F $(^3He,d)$, $E=20$–23 MeV; measured $\sigma(E,\theta)$, deduced S. DWBA and CCBA analysis; $\theta=20$–150°, $\Delta\theta=5°$.]

I. INTRODUCTION

It has been thought for some time now that nuclei in the region of mass 20 are among the most deformed in the entire Periodic Table.[1] Such large deformations lead to large inelastic collective excitation and, in treating transfer reactions among these nuclei, it is necessary to consider transitions connecting states other than the initial and final states. This procedure can alter the cross sections for allowed transitions as well as allowing "forbidden" transitions. In addition, the coherent addition of the many amplitudes involved is a severe test of the nuclear wave functions used to generate them.

In the present work, angular distributions of deuteron groups populating the low-lying states of ^{20}Ne from the $^{19}F(^3He,d)^{20}Ne$ reaction at 21- and 23-MeV bombarding energy have been measured. In addition, limited excitation functions at $\theta_{lab}=25$ and 45° have been measured, confirming the predominantly direct nature of the reaction.

In Sec. IV, the angular distributions of deuteron groups from the states in ^{20}Ne forming the five lowest rotational bands are analyzed in terms of the distorted-wave Born approximation (DWBA) and also in terms of the coupled-channel Born approximation (CCBA) with explicit coupling among members of a band in both the entrance and exit channels.

II. EXPERIMENTAL PROCEDURE

The Florida State University super FN tandem Van de Graaff in conjunction with a closed ^3He recovery system was used to accelerate $^3He^-$ ions with beam currents of 100–300 nA. The targets consisted of CaF_2 sandwiched by evaporation between a thin carbon deposit and a thin flash of gold. The deuteron groups from ^{19}F, which are some 10 MeV more energetic than those from all the other even-A contaminants in the target, were detected by two E-ΔE cooled counter telescopes, consisting of 3-mm Si(Li) E detectors and 300–400-μm totally depleted Si surface-barrier transmission counters. The identifier circuit initially consisted of an ORTEC model 423 particle identifier but was later replaced by an on-line computer system using a particle-identification program.[2] A sample spectrum can be seen in Fig. 1.

The total target thickness was approximately 50-keV to 21-MeV ^3He, and the over-all resolution was about 100 keV. The absolute normalization of the data was determined by scattering 9-MeV ^3He and 6-MeV α particles from the calcium on the target at forward angles (the fluorine peak could not be resolved from contaminant oxygen on the target). The assumed ratio of two F atoms to one Ca atom was checked to be accurate to ±5% by comparing measured $^{19}F(^3He,d)^{20}Ne$ cross sections at 10 MeV with the cross sections of Siemssen, Lee, and Cline.[3]

Relative uncertainties, shown on the data in Figs. 2–7, are a combination of the statistical error, peak-fitting error where applicable, and over-all repeatability where data was repeated. The standard deviation on the over-all normalization, determined by Rutherford scattering and the comparison discussed above, is ±10%.

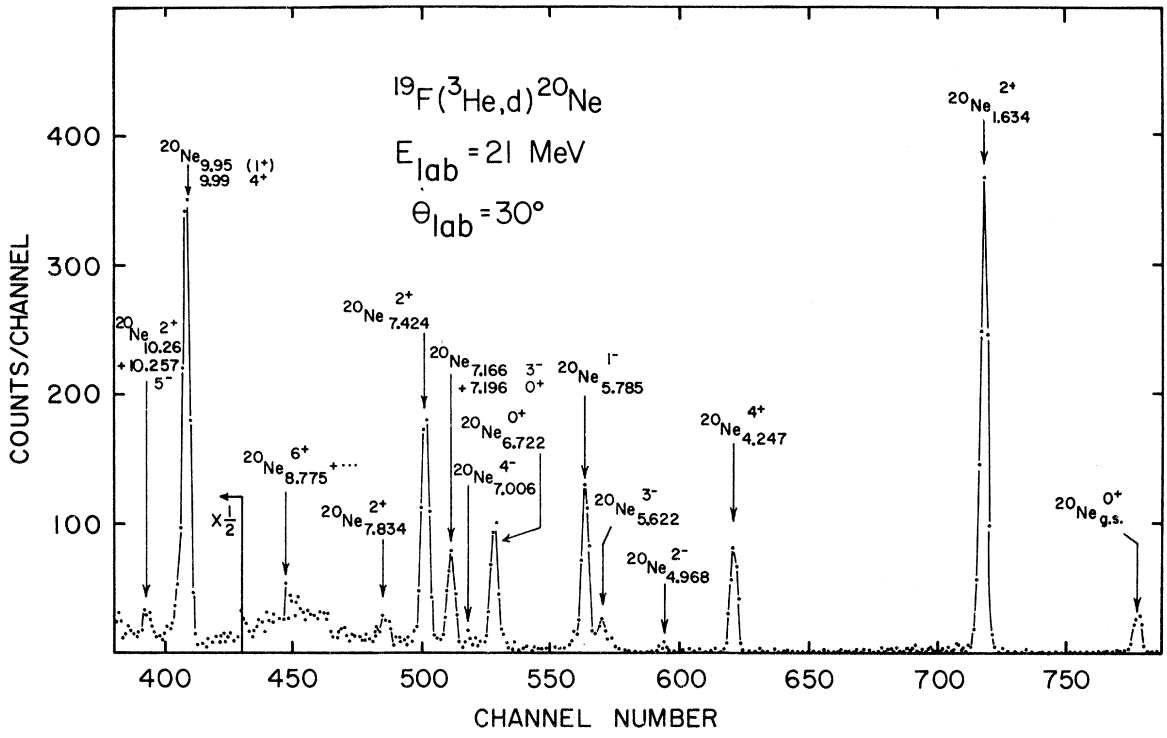

FIG. 1. Energy spectrum for the $^{19}F(^{3}He,d)^{20}Ne$ reaction.

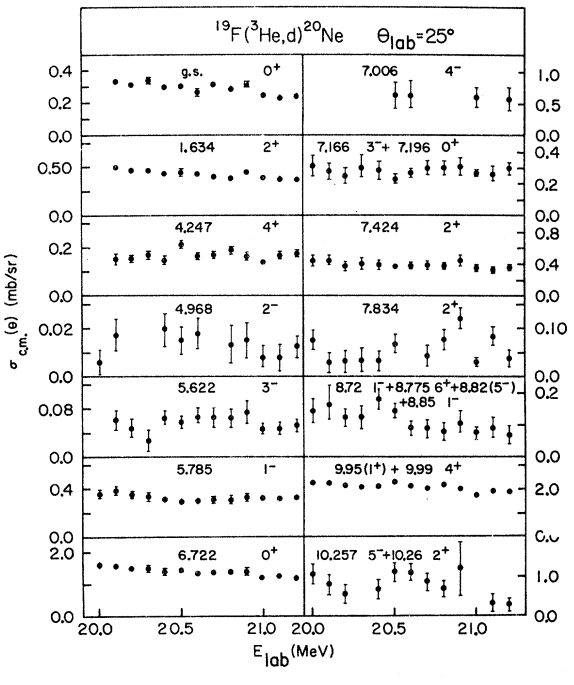

FIG. 2. Measured excitation functions for the ^{19}F-$(^{3}He,d)^{20}Ne$ reaction at 25°.

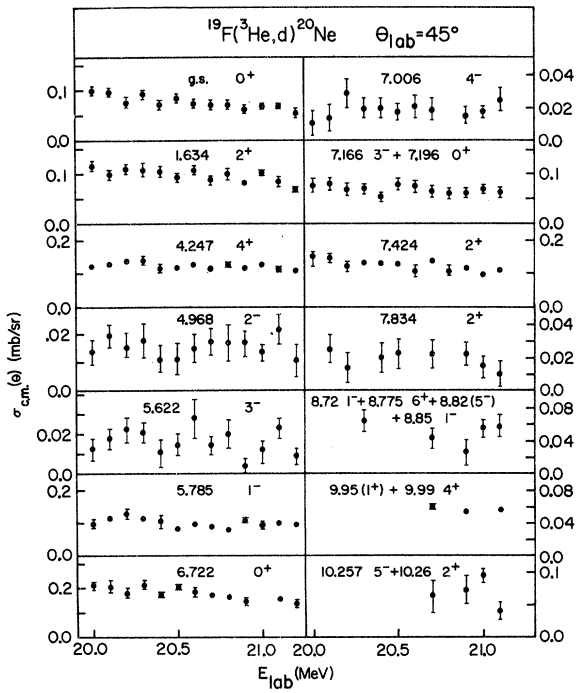

FIG. 3. Measured excitation functions for the ^{19}F-$(^{3}He,d)^{20}Ne$ reaction at 45°.

III. EXPERIMENTAL RESULTS

As seen in Fig. 1, at the forward angles up to 14 deuteron groups populating levels in ^{20}Ne were observed. Due to the presence of contaminant deuteron groups above approximately 10 MeV excitation in ^{20}Ne, only deuteron groups in ^{20}Ne up to the 10.257–10.26-MeV doublet could be identified reliably. At backward angles poor statistics prevented the identification of some of the higher states in ^{20}Ne. The deuteron groups seen in Fig. 1 can be identified with the first five rotational bands[4–7] in ^{20}Ne, shown in Fig. 8. The particle-hole configurations indicated are mainly for identification and do not necessarily exclude other possible configurations.

Limited excitation-function measurements were made at two forward angles (25 and 45°) since it is there that the direct-reaction theory as used here is expected to be most valid. As can be seen in Figs. 2 and 3, the data appear to be reasonably smooth, indicating probably little compound contribution. Such a criterion at backward angles is less meaningful since there nondirect effects might be more important. An estimate of the compound contribution using Hauser-Feshbach theory,[8] when normalized to agree with the smallest cross section observed, in fact gives a negligible contribution to the remainder of the data. As further evidence for the absence of compound effects, the 4.968-MeV (2^-) cross section is seen to be fairly large and nearly symmetric about 90° at 10-MeV bombarding energy. At 21 MeV the 2^- cross section is seen to be fairly small, as it should be if it is produced by a compound reaction. Unfortunately, this cannot be readily distinguished from the coherent addition of many amplitudes contributing to a weak $1p_{1/2}$ hole excitation (see Sec. IV).

The 4.247-MeV (4^+) transition, which is forbidden by angular momentum conservation requirements assuming transfer of a particle into an *s-d* orbit, is, however, seen to be fairly strong, even more so at the backward angles relative to the ground-state (0^+) and 1.634-MeV (2^+) transitions. Since the $1g_{9/2}$ contribution can be estimated from deformed bound-state calculations (Sec. IV) to be less than 3%, and in view of the large deformations[9] around ^{20}Ne, the current work assumes multistep processes are responsible for the large 4.247-MeV 4^+ cross section, as indicated schematically in Fig. 9. Here for illus-

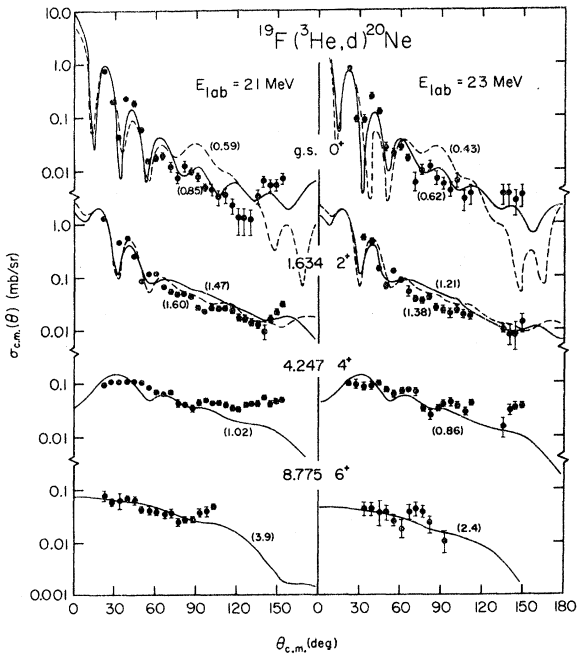

FIG. 4. Measured angular distributions for the states in the ground-state $K=0^+$ band in ^{20}Ne with the ^{19}F(^{3}He,d)^{20}Ne reaction at 21 and 23 MeV. DWBA predictions are indicated by dashed lines and CCBA predictions are indicated by solid lines. The numbers in parentheses indicate the renormalization of theory to experiment forward of 60°.

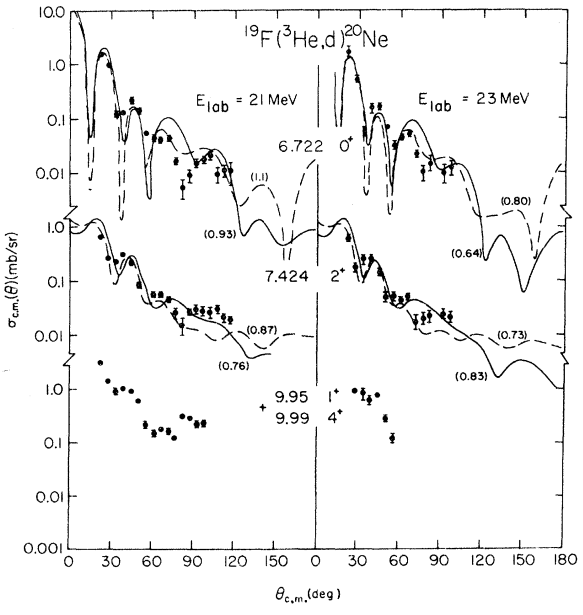

FIG. 5. Measured angular distributions for the states in the 6.722 $K=0^+$ band in ^{20}Ne with the ^{19}F(^{3}He,d)^{20}Ne reaction at 21 and 23 MeV. DWBA predictions are indicated by dashed lines and CCBA predictions are indicated by solid lines. The numbers in parentheses indicate the renormalization of theory to experiment forward of 60°.

tration the first three members of the ground-state bands in ^{19}F and ^{20}Ne are shown coupled through inelastic excitation, leading to 14 possible transitions within the s-d shell. A similar analysis has successfully described the "j-forbidden" ^{24}Mg(d, p)^{25}Mg 1.611-MeV $\frac{7}{2}^+$ transition,[10] which is also characterized by a large cross section and a structureless angular distribution.

IV. DWBA AND CCBA ANALYSIS

Both DWBA and CCBA calculations in the present work were carried out with the code MARS.[11] For the CCBA calculations coupling through inelastic collective excitations is assumed. For this reason transition amplitudes were calculated from the Nilsson model,[12] using solutions of bound-state deformed-well calculations obtained with the code NEPTUNE.[13] The use of shell-model spectroscopic amplitudes,[14] even with collective-model phases, with collective inelastic excitation is open to severe question[15] since the relative phases of the scattering wave functions are determined from the D matrix while the shell model does not have a D matrix in it. True consistency can occur only when shell-model amplitudes are used with inelastic excitations which are also generated from a shell model.

Optical-model parameters in the entrance channel are available[16] for the scattering of 22.4-MeV ^{3}He from ^{19}F. Although no data exist for the inelastic scattering of ^{3}He from ^{19}F, Kemper, Haynes, and Fletcher[17] have measured the inelastic scattering of ^{3}He from ^{20}Ne at 17.83 MeV. In the present experiment the ground state ($\frac{1}{2}^+$), 0.197-MeV ($\frac{5}{2}^+$), and 1.557-MeV ($\frac{3}{2}^+$) states in ^{19}F were coupled together in the CCBA calculations. If the $\frac{3}{2}^+$ and $\frac{5}{2}^+$ states in ^{19}F can be considered as a proton hole coupled to the 2^+ state in ^{20}Ne at 1.634 MeV, then the same inelastic scattering parameters that describe the 0^+-2^+ excitation in ^{20}Ne should describe the $\frac{1}{2}^+$-$\frac{3}{2}^+$-$\frac{5}{2}^+$ excitation in ^{19}F. The optical-model parameters of Oh *et al.*[16] for the elastic scattering of 22.4-MeV ^{3}He from ^{19}F (Table I) do in fact reproduce reasonably well the 0^+-2^+ excitation (using the JUPITOR-1 code[18]) of ^{20}Ne by 17.83-MeV ^{3}He as measured by Kemper, Haynes, and Fletcher[17] with only a β_2 deformation of 0.45. Reducing the absorption from the elastic value does not further improve the ^{20}Ne 0^+-2^+ fit. It was felt sufficient to explicitly include only the first three members of the $K=\frac{1}{2}^+$ ground-state

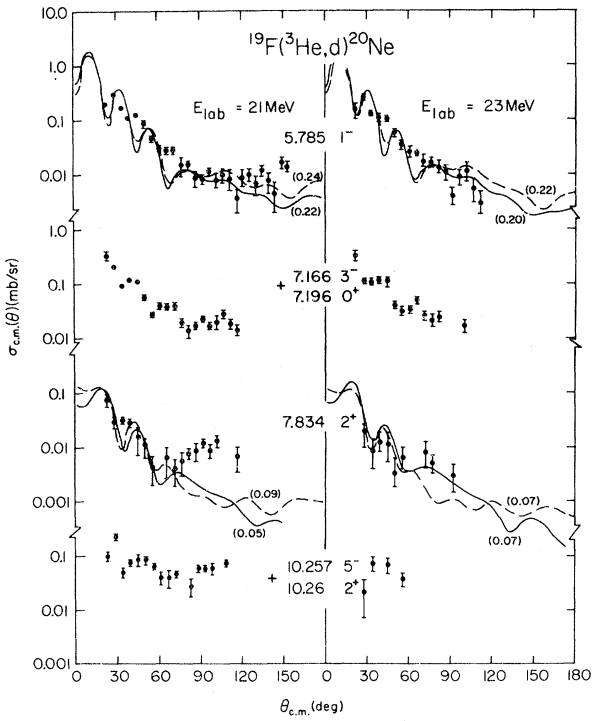

FIG. 6. Measured angular distributions for the states in the $K=0^-$ band and the 7.196-MeV $K=0^+$ band in ^{20}Ne with the ^{19}F(^{3}He, d)^{20}Ne reaction at 21 and 23 MeV. DWBA predictions are indicated by dashed lines and CCBA predictions are indicated by solid lines. The numbers in parentheses indicate the renormalization of theory to experiment forward of 60°.

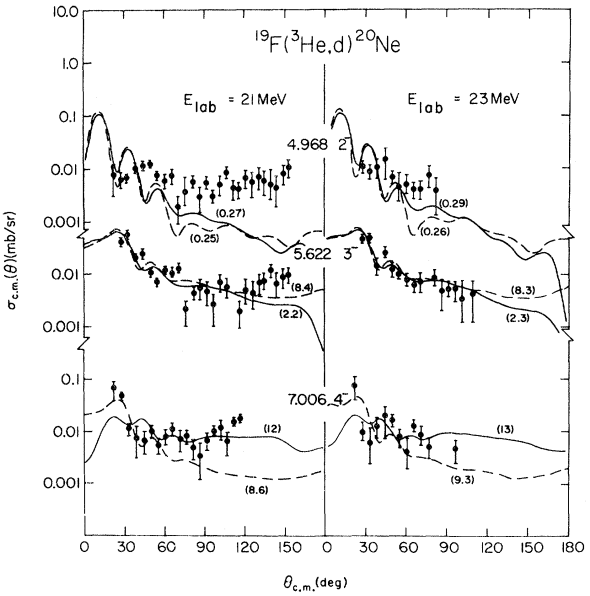

FIG. 7. Measured angular distributions for the states in the 4.968-MeV $K=2^-$ band in ^{20}Ne with the ^{19}F(^{3}He, d)-^{20}Ne reaction at 21 and 23 MeV. DWBA predictions are indicated by dashed lines and CCBA predictions are indicated by solid lines. The numbers in parentheses indicate the renormalization of thoery to experiment forward of 60°.

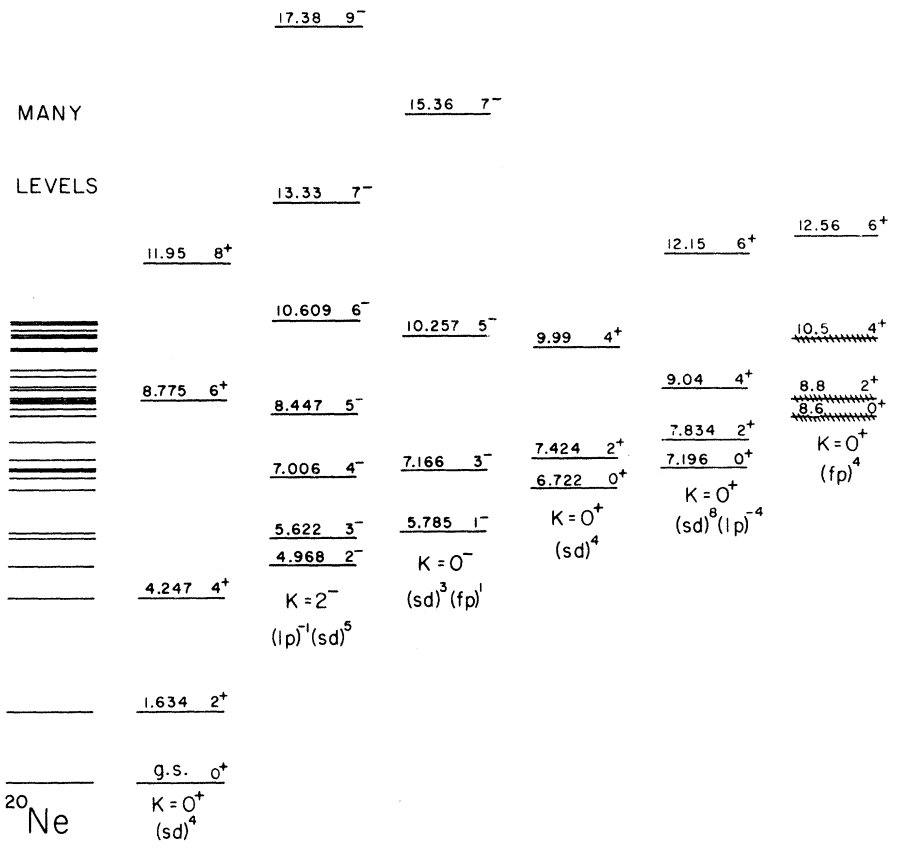

FIG. 8. Decomposition of observed spectra in ^{20}Ne into rotational bands.

band in ^{19}F for the CCBA calculations, since the scattering from ^{19}F of 15-MeV deuterons by Dienhard and Hintz[19] and 30-MeV protons by De Swiniarski *et al.*[20] shows these three states to be most strongly populated, with excitation to the $K=\frac{1}{2}^-$ band as well as to higher-spin states belonging to the ground-state $K=\frac{1}{2}^+$ band typically an order of magnitude weaker.

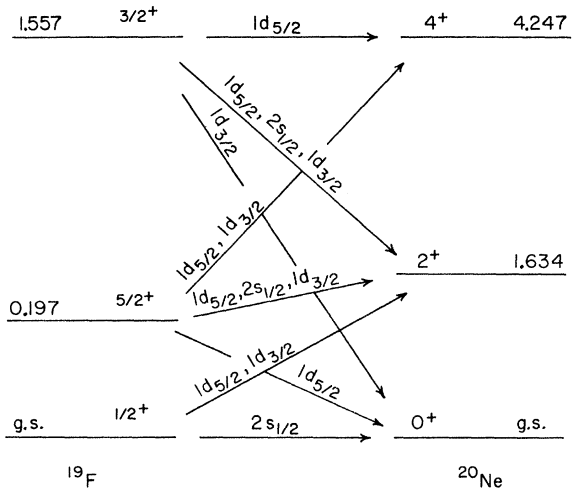

FIG. 9. Allowed transitions among the lowest three members of the ground-state bands of ^{19}F and ^{20}Ne through $l=2$ and $l=0$ for the ^{19}F(^{3}He, d)^{20}Ne reaction.

The outgoing deuterons in the present experiment have energies in the range 20–30 MeV. The deuteron optical-model parameters used in the present analysis and listed in Table I are similar to those of Siemssen, Lee, and Cline[3] used at lower energies. The present parameters were determined by fitting the elastic-inelastic scattering data of Hinterberger *et al.*[21] at $E_d=52$ MeV. Meyer *et al.*[22] have also measured the elastic scattering of 28-MeV deuterons from ^{20}Ne. However, their analysis included spin-orbit coupling, while in the present work spin-orbit coupling was ignored in the entrance and exit channels, and also their data was not readily available for reanalysis. The present deuteron parameters and those of Hinterberger *et al.*[21] and Meyer *et al.*[22] can be seen[14] to be related through a continuous Vr^n ambiguity; however, the present choice of parameters was best able to fit the ^{19}F(^{3}He, d)^{20}Ne data. The resulting fits to the 52-MeV deuteron 0^+-2^+-4^+

TABLE I. Optical-model parameters in entrance, exit, and bound-state channels.

Parameter set	Channel	V [a] (MeV)	r_0 (fm)	a_0 (fm)	W (MeV)	W_D (MeV)	r_i (fm)	a_i (fm)	r_c (fm)	V_{so} (MeV)	β_2	β_4
A	^{3}He+^{19}F DWBA	177.	1.08	0.73	17.4	0.	1.73	0.80	1.4	0.	0.	0.
B	^{3}He+^{19}F CCBA	177.	1.08	0.73	17.4	0.	1.73	0.80	1.4	0.	0.45	0.
C	d+^{20}Ne DWBA	100.	1.0	0.9	0.	11.	1.5	0.8	1.3	0.	0.	0.
D	d+^{20}Ne CCBA	100.	1.0	0.9	0.	10.	1.5	0.8	1.3	0.	0.45	0.15
E	p+^{19}F DWBA	···	1.25	0.65	···	···	···	···	1.25	7.5	0.	0.
F	p+^{19}F CCBA	···	1.25	0.65	···	···	···	···	1.25	7.5	0.45	0.

[a] Adjusted to fit the appropriate separation energies for the bound-state channel.

excitation in ^{20}Ne (W = 10 MeV) and elastic only (W = 11 MeV) as well as the 0^+-2^+ excitation in ^{24}Mg by 21-MeV deuterons[14] were reasonably good. It is interesting to note that although the scattering of 17.83-MeV ^{3}He requires no β_4 deformation[15] to explain the 0^+-2^+-4^+ excitation in ^{20}Ne, a β_4 deformation[20] is necessary to reproduce the 4^+ scattering data by 52-MeV deuterons. Average[9,20] deformation parameters of β_2 = 0.45 and β_4 = 0.15 were used for the deuteron channel in the present CCBA analysis.

The bound-state calculations were performed with the code NEPTUNE using standard parameters (Table I) for a proton in ^{20}Ne with a spherical potential (β_2 = 0) for the DWBA calculations and a deformed potential (β_2 = 0.45) for the CCBA calculations. In the CCBA calculations spherical form factors were also tried with the proper separation energy for each amplitude. These gave essentially the same shapes to the angular distributions as the deformed form factors and a difference in magnitude of less than 20%. In the present work only deformed form factors are used in the CCBA calculations.

Transition amplitudes were calculated using the Nilsson model with the expression[23]

$$\sqrt{S} = g\left(\frac{2I_i+1}{2I_f+1}\right)^{1/2}\langle I_i j K_i\, K_f - K_i | I_f K_f\rangle C_{nlj}\,. \tag{1}$$

Here S is the spectroscopic factor; I_i and I_f are the spins of the initial and final states, respectively; K_i and K_f are their K quantum numbers; j is the total angular momentum of the captured particle; the C_{nlj} are the expansion coefficients of the deformed wave function; and

$$g = (1+\delta_{K_i,0}+\delta_{K_f,0})^{1/2}\,. \tag{2}$$

In addition, the amplitudes given by (1) must be divided by $\sqrt{2}$ for states belonging to other than the ground-state band, since for a T_z = 0 nucleus neutron and proton excitations are indistinguishable.

TABLE II. Mixing coefficients $C_{j\Omega}$ as obtained from deformed-well calculations [E_b = 12.844 − E_{bh} (MeV)].

j \ Ω^π (orbit), E_{bh} (MeV)	$\frac{1}{2}^+$ (6) 0.	$\frac{1}{2}^-$ (4) 4.968	$\frac{1}{2}^-$ (14) ~5.52	$\frac{1}{2}^+$ (9) 6.722	$\frac{1}{2}^+$ (11) 7.196
$\frac{1}{2}$	0.545	−0.917	−0.310	0.514	0.521
$\frac{3}{2}$	0.227	−0.369	0.692	0.676	0.671
$\frac{5}{2}$	−0.807	0.125	0.169	0.527	0.528
$\frac{7}{2}$	0.	0.086	−0.629	0.	0.

The expansion coefficients C_{nlj}, obtained with the code NEPTUNE and listed in Table II, correspond in phase to asymptotically positive bound-state wave functions. An additional phase of i^l (i^{l+1} for odd shells) is included in Table II since the code NEPTUNE obeys the Condon and Shortley phase convention, while the stripping cross sections were calculated with the code MARS, which obeys the time-reversal phase convention.[24] The first three $K = 0^+$ bands were assumed to consist of a proton in Nilsson orbits 6, 9, and 11, respectively. Negative-parity solutions were chosen to correspond to $1p$ shell excitation for the $K = 2^-$ band and $1f$-$2p$ shell excitations for the $K = 0^-$ band.

Both DWBA and CCBA calculations were performed in zero range with the faster version of the code MARS, appropriately modified for odd-A targets. The amplitudes used as input to the code MARS are listed in Table III. For the CCBA calculations the first three members of a given band were explicitly coupled, although the 4^+ member of the third $K = 0^+$ band was not observed. Also, the 5^- member of the $K = 0^-$ band is not resolved from the 10.26-MeV 2^+ T = 1 state and the 4^+ member of the second $K = 0^+$ band is not resolved from the 9.95 (1^+) level. For the DWBA calculations only the direct transitions A_j for $\frac{1}{2}^+ \to J^\pi$ of Table III with spherical form factors were used.

Measured angular distributions at 21 and 23 MeV along with DWBA and CCBA predictions are shown in Figs. 4–7. The numbers in parentheses indicate the renormalization of the angle-inte-

grated theory to the data forward of 60°. In addition, the CCBA predictions for the $K=0^+$ 6.722-MeV band were further increased by 50% to improve the over-all fit at the maxima in the oscillations (see below).

$K=0^+$ Ground-State Band

Both cluster transfer experiments[5,25] and shell-model calculations[26,27] indicate that the members of this rotational band occupy mostly the lowest

TABLE III. Stripping spectroscopic amplitudes A_j determined from the collective model [$A_j=(2s_a+1)^{1/2}S^{1/2}$, where s_a is the projectile spin and S is the spectroscopic factor].

Ω^π (orbit)	E_x (MeV)	J^π	K^π	$l(j)=1(\frac{1}{2})$	$0(\frac{1}{2})$	$1(\frac{3}{2})$	$2(\frac{3}{2})$	$3(\frac{5}{2})$	$2(\frac{5}{2})$	$3(\frac{7}{2})$
					A_j for $\frac{1}{2}^+\rightarrow J^\pi$					
$\frac{1}{2}^+$ (6)	0.	0^+	0^+		1.090		0.		0.	
	1.634	2^+			0.		0.203		−0.722	
	4.247	4^+			0.		0.		0.	
$\frac{1}{2}^-$ (4)	4.968	2^-	2^-	0.		−0.233		0.032		0.
	5.622	3^-		0.		0.		0.061		0.023
	7.006	4^-		0.		0.		0.		0.035
$\frac{1}{2}^-$ (14)	5.785	1^-	0^-	−0.253		0.565		0.		0.
	7.166	3^-		0.		0.		0.090		−0.336
	10.257	5^-		0.		0.		0.		0.
$\frac{1}{2}^+$ (9)	6.722	0^+	0^+		0.727		0.		0.	
	7.424	2^+			0.		0.427		0.333	
	9.99	4^+			0.		0.		0.	
$\frac{1}{2}^+$ (11)	7.196	0^+	0^+		0.737		0.		0.	
	7.834	2^+			0.		0.424		0.334	
	9.04	4^+			0.		0.		0.	
					A_j for $\frac{3}{2}^+\rightarrow J^\pi$					
$\frac{1}{2}^+$ (6)	0.	0^+	0^+		0.		−0.454		0.	
	1.634	2^+			0.689		0.203		0.386	
	4.247	4^+			0.		0.		−0.704	
$\frac{1}{2}^-$ (4)	4.968	2^-	2^-	0.		0.233		−0.069		−0.023
	5.622	3^-		0.		−0.197		−0.027		−0.040
	7.006	4^-		0.		0.		0.061		−0.006
$\frac{1}{2}^-$ (14)	5.785	1^-	0^-	−0.358		−0.253		−0.151		0.
	7.166	3^-		0.		0.496		0.081		0.194
	10.257	5^-		0.		0.		0.		−0.346
$\frac{1}{2}^+$ (9)	6.722	0^+	0^+		0.		−0.956		0.	
	7.424	2^+			0.460		0.427		−0.178	
	9.99	4^+			0.		0.		0.325	
$\frac{1}{2}^+$ (11)	7.196	0^+	0^+		0.		−0.949		0.	
	7.834	2^+			0.466		0.424		−0.178	
	9.04	4^+			0.		0.		0.326	
					A_j for $\frac{5}{2}^+\rightarrow J^\pi$					
$\frac{1}{2}^+$ (6)	0.	0^+	0^+		0.		0.		−1.614	
	1.634	2^+			0.844		−0.133		0.772	
	4.247	4^+			0.		0.243		−0.498	
$\frac{1}{2}^-$ (4)	4.968	2^-	2^-	0.		−0.153		0.078		0.046
	5.622	3^-		0.		0.242		−0.033		0.023
	7.006	4^-		0.		−0.180		−0.043		−0.030
$\frac{1}{2}^-$ (14)	5.785	1^-	0^-	0.		−0.758		0.040		−0.582
	7.166	3^-		−0.287		0.405		−0.066		0.336
	10.257	5^-		0.		0.		0.111		−0.227
$\frac{1}{2}^+$ (9)	6.722	0^+	0^+		0.		0.		0.745	
	7.424	2^+			0.563		−0.280		−0.356	
	9.99	4^+			0.		0.511		0.230	
$\frac{1}{2}^+$ (11)	7.196	0^+	0^+		0.		0.		0.747	
	7.834	2^+			0.571		−0.278		−0.357	
	9.04	4^+			0.		0.507		0.230	

TABLE IV. Spectroscopic results of the ^{19}F(^{3}He,d)^{20}Ne reaction and predictions of the models.

E_x (MeV)	J^π	C^2S from present study [a] DWBA	CCBA	C^2S from other work (^{3}He,d) [b] (10 MeV)	(d,n) [c] (3 MeV)	Collective model [d] K^π	C^2S	Shell model [e] C^2S
0.	0^+	0.30	0.43	0.31	0.62	0_1^+	0.59	0.72
1.634	2^+	0.42	0.38	0.62	0.70	0_1^+	0.28	0.43
4.247	4^+	0.0	0.0	≤0.21		0_1^+	0.0	0.
4.968	2^-	0.008	0.008	≤0.06		2^-	0.03	
5.622	3^-	0.017	0.004	≤0.042		2^-	0.002	
5.785	1^-	0.044	0.040	0.051		0^-	0.19	0.006
6.722	0^+	0.25	0.22	0.47	0.38	0_2^+	0.26	0.48
7.006	4^-	0.009	0.012	≤0.026		2^-	0.001	
7.166	3^-			≤0.092		0^-	0.06	
7.196	0^+			≤0.027		0_3^+	0.27	0.004
7.424	2^+	0.12	0.12	0.16		0_2^+	0.15	0.11
7.834	2^+	0.012	0.009			0_3^+	0.15	5×10^{-5}

[a] Here $C^2S = \bar{N}(\sum A_j^2)/(2s_a+1)$, where $\bar{N}$ is the energy-averaged renormalization of the theoretical predictions indicated in Figs. 4–7. The A_j are the direct transition spectroscopic amplitudes in Table III.

[b] Reference 3.

[c] Reference 26.

[d] $C^2S = \sum A_j^2/(2s_a+1)$, where the A_j are the direct transition spectroscopic amplitudes listed in Table III.

[e] References 24 and 25.

configurations in the s-d shell. Shell-model spectroscopic factors, assuming active particles in the $1p_{1/2}$-$1d_{5/2}$-$2s_{1/2}$ shells,[26,27] are listed in Table IV for comparison with the experimental values of this and other[3,28] work, and also with those of the collective model. Both DWBA and CCBA spectroscopic factors were calculated from the direct transitions $\frac{1}{2}^+ \rightarrow J^\pi$ of Table III.

The effect of optical-model parameter variation on the spectroscopic factors was studied, and it was possible to get better fits for the ground state both with DWBA and CCBA, for example, by increasing the deuteron imaginary diffuseness or imaginary potential, with a resulting renormalization closer to 1.0. However, the fits to the elastic-inelastic scattering data then deteriorate. It is in fact not at all clear that the same parameters describing the elastic-inelastic channels should be expected to describe the reaction channels, since the two processes may not be occurring in the same region of space. This is in addition to the unavailability of scattering data from excited states. Alternatively, one may hope that the use of folded potentials will give a consistent picture of both scattering and reaction phenomena.[29] Nevertheless, the quality of the CCBA fit is noticeably superior to the DWBA fit for this level. Calculations done with the ^{3}He potential family[17] $V \sim 130$ MeV gave a poor fit to the data and were not pursued.

The 2^+ state at 1.634 MeV is better reproduced with the present parameters, and the extracted spectroscopic factors are in good agreement with theory and, in particular, with the shell model. Both CCBA and DWBA predictions appear to fit equally well for this level.

As discussed earlier, direct DWBA transitions are forbidden to the 4.247-Me 4^+ state within the s-d shell (Fig. 9). The CCBA fits to the data in Fig. 4 for this state are quite good at the forward angles and fall below the data at backward angles.

The 6^+ state at 8.775 MeV in ^{20}Ne is barely discernible among the broad states belonging to the fourth positive-parity band at that energy (Figs. 1 and 8), and the data shown in Fig. 4 for this state are therefore believed to be accurate to within a factor of 2. From the three states considered in the entrance channel, there are no direct transitions to the 6^+ level within the s-d shell. Within the present scheme, this state can therefore only be reached by inelastic excitation through 0^+-2^+-4^+-6^+ coupling. The renormalization of the resultant CCBA calculations, shown in Fig. 4, is not unreasonable, in view of the uncertainty in the data discussed above. Furthermore, transitions through the $\frac{7}{2}^+$-$\frac{9}{2}^+$ members of the $K = \frac{1}{2}^+$ ground-state band in ^{19}F may be important for this level.

Both data and theory in Fig. 4 show rather strikingly well oscillations that become more quenched with increasing final spin. For the 0^+ and 2^+ levels, where the direct transitions dominate at

the forward angles, characteristic $l=0$ and $l=2$ stripping patterns, respectively, can be seen. The 4^+ and 6^+ levels, on the other hand, are dominated almost entirely by multistep processes, and here the angular distributions are structureless.

$K=0^+$ 6.722-MeV Band

This band is also mainly an s-d shell band.[5,25-27] The experimental spectroscopic factors for the 0^+ state at 6.722 MeV (Fig. 5) are in good agreement with the collective model, and there is evidence[27] that inclusion of the $1d_{3/2}$ shell in the shell-model calculation would decrease C^2S by about 30%, and therefore be in reasonable agreement with the experimental and collective-model results. Here again there is some difficulty in fitting the data, especially in phase, and the remarks made in the previous section may equally well apply, although in this band two particle excitations out of the $1p_{1/2}$ shell are becoming important.[26,27]

The experimental spectroscopic factors for the 2^+ level at 7.424 MeV are in good agreement with both the collective and shell models. The quality of the CCBA vs DWBA predictions, as for the 0^+ state, are about the same and both show characteristic stripping patterns for $l=2$ and 0, respectively.

The 4^+ member of this band at 9.99 MeV could not be resolved from a 1^+ level at 9.95 MeV, and therefore no predictions are shown, although an $l=2$ stripping component can be seen in the 21-MeV data for this doublet.

$K=0^+$ 7.196-MeV Band

Cluster transfer experiments[5,25] suggest that this is predominantly an 8p-4h band while shell-model calculations for the 0^+ state at 7.196 MeV, for example, indicate only 26% 8p-4h configurations and 35% 6p-2h configurations, with similar results for the 2^+ state at 7.834 MeV.[26,27] Since in the present work the 0^+ state at 7.196 MeV could not be resolved from the 3^- state at 7.166 MeV, no predictions are shown in Fig. 6 although an $l=0$ component in the shape can be seen. The experimental spectroscopic factor for the 2^+ state at 7.834 MeV is seen to be much smaller than the collective-model value, which is consistent with a many-particle configuration for this state. The shell-model spectroscopic factors for this band on the other hand are too small, perhaps because the predicted levels lie too high in excitation energy compared to the observed levels.[26,27] Both CCBA and DWBA curves fit reasonably well at the forward angles but drop off too quickly at backward angles. This is characteristic of the fact that too few amplitudes (e.g., corresponding to many-particle configurations) have been included.

$K=2^-$ 4.968-MeV Band

The states in this band are seen in Fig. 1 to be weakly populated, compared with the negative-parity states in the $K=0^-$ band (Fig. 8). This plus cluster transfer data[5,25] suggest that the band consists mainly of $1p_{1/2}$ hole excitations, rather than excitation into the $1f_{7/2}$ shell. This is further supported by the fact that every other state in this band (Fig. 8) has unnatural parity.[25] The states in this band should, in contrast, be well populated in pickup reactions, and in fact the ^{22}Ne$(p, t)^{20}$Ne reaction to levels in the $K=2^-$ band is well described by CCBA theory.[30]

The quality of the CCBA vs DWBA predictions is about the same for all three levels, as seen in Fig. 7. The agreement of the extracted spectroscopic factors with the predictions of the collective model is quite poor, with the exception of the CCBA result for the 3^- level at 5.622 MeV. The ratio of the observed to the predicted spectroscopic factors can be seen to increase with increasing spin, suggesting a compound contribution to the observed cross sections, where $\sigma_{CN} \sim 2J+1$. The lack of structure and apparent symmetry about 90° further supports this conclusion. Since only $p_{1/2}$ excitations are considered here in the shell model, no spectroscopic factors are available.

$K=0^-$ Band

The strong transitions in the present experiment (Fig. 1) and cluster transfer data[5,23] indicate that this band consists mainly of transitions into the $1f_{7/2}$ shell. CCBA and DWBA predictions for the 1^- state at 5.785 MeV, the only one resolved, are shown in Fig. 6. The discrepancy between theory and experiment might in part be due to the fact that the next deeper NEPTUNE solution after the $1f$-$1p$ solution, which was used for the $K=2^-$ band (Table II), is a $1f$-$2p$ solution. This solution seems to give too much weight to the $2p$ shell. The $1p_{1/2}$ spectroscopic factor from the shell model (Table IV) on the other hand seems to give too little strength. Both CCBA and DWBA predictions to this level are of about the same quality.

V. CONCLUSION

The DWBA theory is seen to give an adequate representation of the data for the "allowed" transitions. Assignments of l values are consistent with the work of Siemssen *et al.*[3,28] at lower energies. Extracted spectroscopic factors for the most part seem to agree over a large range of

energies, although the sensitivity of the spectroscopic factors in the present work to the optical-model parameters is in many cases quite severe.

The CCBA calculations in general give better fits to the allowed positive-parity transitions than the DWBA, and explain quite well the excitation of "j-forbidden" states. However, it appears the collective-model CCBA theory for single-nucleon stripping reactions is at best a limited test of nuclear wave functions, due to the sensitivity of the calculations to optical-model parameters. The negative-parity transitions are not as well reproduced as the positive-parity states by either the DWBA or CCBA theories, probably due to the more complex configurations of the former.

ACKNOWLEDGMENTS

The authors would like to acknowledge L. Rowton and Dr. D. L. McShan for invaluable help with the ^{3}He recovery system and particle-identification computer system, respectively. We are also indebted to Professor T. Udagawa and Professor W. R. Coker for providing us with the MARS and NEPTUNE programs, respectively, and Professor T. Udagawa, Professor D. Robson, and Dr. R. de Meijer for many helpful discussions.

---

*Work supported in part by the National Science Foundation Grants Nos. NSF-GU-2612 and NSF-GP-25974.

†Present address: Physics Department, University of Texas, Austin, Texas 78712.

[1]M. C. Mermaz, C. A. Whitten, Jr., and D. A. Bromley, Phys. Rev. 187, 1466 (1969).

[2]D. L. McShan, private communication.

[3]R. H. Siemssen, L. L. Lee, Jr., and D. Cline, Phys. Rev. 140, B1258 (1965).

[4]A. E. Litherland, J. A. Keuhner, H. E. Gove, M. A. Clark, and E. Almquist, Phys. Rev. Lett. 7, 98 (1961).

[5]H. T. Fortune, in Proceedings of Heavy Ion Conference, CONF 720669, Oak Ridge, Tennessee, 1972 (unpublished), p. 353.

[6]A. D. Panagiotou, J. C. Cornell, N. Anyas-Weiss, P. N. Hudson, A. Menchaca-Rocha, D. K. Scott, J. Becker, and B. E. F. Macefield, Bull. Am. Phys. Soc. 18, 136 (1973).

[7]F. Ajzenberg-Selove, Nucl. Phys. A190, 1 (1972).

[8]K. A. Eberhard, P. Von Brentano, M. Böhning, and R. O. Stephen, Nucl. Phys. A125, 673 (1969).

[9]H. Rebel, G. W.Schweimer, G. Schatz, J. Specht, R. Löhken, G. Hauser, D. Habs, and H. Klewe-Nebenius, Nucl. Phys. A182, 145 (1972).

[10]D. Braunschweig, T. Tamura, and T. Udagawa, Phys. Lett. 35B, 273 (1971).

[11]T. Tamura and T. Udagawa, University of Texas Report No. 30, 1972 (unpublished).

[12]S. G. Nilsson, K. Dan. Vidensk. Selsk. Mat.-Fys. Medd. 29, 16 (1955).

[13]T. Tamura, University of Texas Report Neptune, 1971 (unpublished).

[14]R. O. Nelson and N. R. Roberson, Phys. Rev. C 6, 2153 (1972).

[15]D. Robson, private communication.

[16]K. Oh, C. S. Zaidins, C. D. Zafiratos, and S. I. Hayakawa, Nucl. Phys. A178, 497 (1972).

[17]K. W. Kemper, D. S. Hayes, and N. R. Fletcher, Phys. Rev. C 4, 108 (1971).

[18]T. Tamura, Oak Ridge National Laboratory Report No. 4152, 1967 (unpublished).

[19]D. Dehnhard and N. M. Hintz, Phys. Rev. C 1, 460 (1970).

[20]R. De Swiniarski, A. Genoux-Lubain, G. Bagieu, J. F. Cavaignac, and D. H. Worledge, Phys. Lett. 43B, 27 (1973).

[21]F. Hinterberger, G. Mairle, U. Schmidt-Rohr, and G. J. Wagner, Nucl. Phys. A111, 265 (1968); *ibid.* A115, 570 (1968).

[22]J. Meyer, B. Audebert, E. Elbaz, and J. Lafoucrière, C. R. Acad. Sci. B 266, 969 (1968).

[23]G. R. Satchler, Ann. Phys. (N.Y.) 3, 275 (1958).

[24]T. Udagawa, private communication.

[25]N. Marquardt, W. von Oertzen, and R. L. Walter, Phys. Lett. 35B, 37 (1971).

[26]J. B. McGrory and B. H. Wildenthal, Phys. Rev. C 7, 974 (1973).

[27]R. de Meijer, private communication.

[28]R. H. Siemssen, R. Felst, M. Cosack, and J. L. Weil, Nucl. Phys. 52, 273 (1964).

[29]G. R. Satchler, Phys. Rev. C 4, 1485 (1971).

[30]D. K. Olsen, T. Udagawa, T. Tamura, and R. E. Brown, Phys. Rev. Lett. 29, 1178 (1972).